Master Thesis

Signal and background studies for scalar leptoquark pair production in the $t\bar{t} + 2\tau$ channel at the ATLAS experiment

Daniel Adlkofer

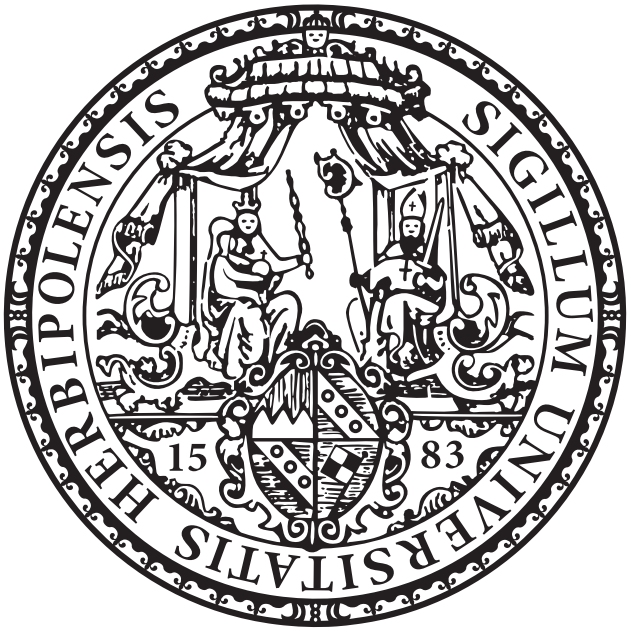

Supervisor
Prof. Dr. Raimund Ströhmer

Advisor
Dr. Mahsana Haleem

December 2018

Physikalisches Institut
Lehrstuhl für Physik und ihre Didaktik
Julius-Maximilians-Universität Würzburg

Contents

1

XyZ

sample	$\mathbf{t\bar{t}}$	$\mathbf{t\bar{t}H}$	$\mathbf{LQ}_{500\,\mathrm{GeV}}$	$\mathbf{LQ}_{1\,\mathrm{TeV}}$
selection	reconstruction	reconstruction	reconstruction	reconstruction
	event yield	event yield	event yield	event yield
≥ 2 b-jets	186 395	209	152	1.5
≥ 2 b-jets + $\geq 1\,\tau$	505	7	94	0.9
≥ 2 b-jets + $\geq 2\,\tau$	1.7	0.4	27	0.2

Table 1.1: Event yield for different selections with tau leptons for the $t\bar{t}$, the $t\bar{t}H$ and the LQ Monte Carlo sample. The luminosity account for $150\,\mathrm{fb}^{-1}$.

sample	$\mathbf{t\bar{t}}$	$\mathbf{t\bar{t}H}$
selection	efficiency $\frac{\epsilon}{\%}$	efficiency $\frac{\epsilon}{\%}$
≥ 2 b-jets	26.52	36.72
≥ 2 b-jets $+1\,\tau$	3.18	8.83
≥ 2 b-jets $+2\,\tau$	1.41	2.13

Table 1.2: Efficiencies for different selections with tau leptons for the $t\bar{t}$ and the $t\bar{t}H$ Monte Carlo sample.

sample		**$t\bar{t}$**		**$t\bar{t}H$**	
selection	reference selection	reconstruction ratio $\frac{r}{\%}$	truth ratio $\frac{r}{\%}$	reconstruction ratio $\frac{r}{\%}$	truth ratio $\frac{r}{\%}$
≥ 2 b-jets $+1\,\tau$	≥ 2 b-jets	0.28	2.35	3.43	14.26
≥ 2 b-jets $+2\,\tau$	≥ 2 b-jets	0.0011	0.020	0.24	4.11

Table 1.3: Ratios for different selections with tau leptons for the $t\bar{t}$ and the $t\bar{t}H$ Monte Carlo sample.

sample	**$t\bar{t}$**		**$t\bar{t}H$**	
selection	numerator event yield	denominator event yield	numerator event yield	denominator event yield
truth matching for tau	63	13723	5590	21610
efficiency	0.46%		25.9%	
tau from H^0, $W^{\pm}$, Z^0	0	0	4859	11988
efficiency	-		40.5%	
tau from B-mesons	63	13722	20	7416
efficiency	0.46%		0.27%	
tau within a jet	8440	3776952	18511	20327225
efficiency	0.22%		0.091%	
tau within a b-jet	6098	2658379	2317	1208924
efficiency	0.23%		0.19%	

Table 1.4: Event yield for different selections with tau leptons for the $t\bar{t}$ and the $t\bar{t}H$ Monte Carlo sample. The luminosity account for 36.1 fb^{-1}.

sample	**LQ**$_{500\,\mathrm{GeV}}$		**LQ**$_{1\,\mathrm{TeV}}$	
selection	numerator event yield	denominator event yield	numerator event yield	denominator event yield
truth matching for tau	2604	5362	2263	5055
efficiency	48.6%		44.8%	
tau from H^0, $W^{\pm}$, Z^0	95	340	82	461
efficiency	27.9%		17.8%	
tau from B-mesons	0	183	0	200
efficiency	0.0%		0.0%	
tau from LQ	1744	3286	1057	2022
efficiency	53.1%		52.3%	
tau within a jet	7232	55208	7011	63671
efficiency	13.1%		11.0%	
tau within a b-jet	2317	1208924	6098	2658379
efficiency	0.45%		0.23%	

Table 1.5

2

Introduction

3

Theoretical background for the search of scalar leptoquarks

3.1 The Standard Model of particle physics

4

Experimental setup for the search of scalar leptoquarks

For the search of scalar leptoquarks the ATLAS detector at the Large Hadron Collider (LHC) is used as experimental setup which will be described within this chapter. In section 4.1 the general setting of the proton-proton collider located at the CERN research center is the subject of interest. The particle detection of the resulting collision events will take place in the ATLAS detector with its different specialized components (section 4.2). Section 4.3 addresses the leptoquark pair production in proton-proton collisions.

4.1 The Large Hadron Collider accelerator complex

The research center CERN (Conseil Européen pour la Recherche Nucléaire) was founded in 1954 near Geneva, Switzerland to become a major European joint venture on elementary particle physics. In the mean time 22 member states are participating in that large-scale project with the ambition to probe the essential constitutes of nature and the fundamental forces acting between them. [1]

In the huge accelerator complex protons reach through different stages energies of 6.5 TeV and will be brought to collisions at defined interaction sites in time intervals of 25 ns. Particle detectors then register signatures of the resulting collsion events and the analysis of new created particles gives insight to the nature of elementary particle physics.
Figure 4.1 shows the different acceleration stages. Starting from the injection protons will gain as much energy as 50 MeV in the linear accelerator LINAC2 and will

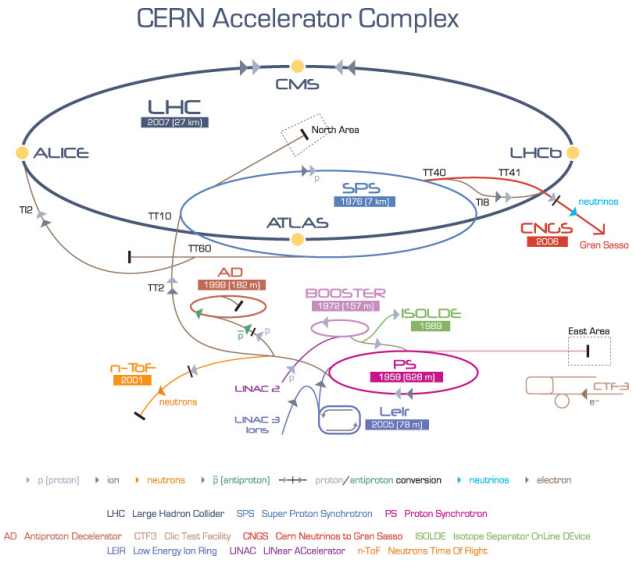

Figure 4.1: Schematic of the CERN accelerator complex with its different stages and few experiments like ATLAS located at one crossing point for protons. [2]

be further transferred to the Proton Synchrotron Booster (1.4 GeV), the Proton Synchrotron (25 GeV), the Super Proton Synchrotron (450 GeV) and finally to the LHC ring with its 26.7 km circumference. [1]
The LHC is designed as two-ring proton-proton collider. Conditions for a stable proton beam are diversely including high vacua of 10^{-10} mbar to 10^{-11} mbar and temperatures of 1.9 K for the superconducting NbTi-magnets of the accelerator. [3]

Different more experiments like ALICE[4], LHCb[5] are located at CERN due to the variety of research questions. But the subject of interest in this work lies in the high luminosity experiment ATLAS specialized for proton-proton collisions like its counterpart CMS[6]. Main tasks of ATLAS are more precise measurements of the SM (see chapter 3.1), better understanding Quantum Chromo Dynamics (QCD) or search for supersymmetric models and new physics. With the LHC production of 109 inelastic events per second up to 23 simultaneously events at dominating high QCD cross sections reqiure a powerful detector that is capable of recognizing the characteristic signatures. These circumstances make up the demands for ATLAS including fast electronic elements, high detector granularity, handling high particles

fluxes and reducing overlapping events at a large acceptance and coverage region. [7]

4.2 The ATLAS detector at the LHC

One of the general purpose detector for proton-proton collisions is the ATLAS detector. This 25 m tall detector is located at one interaction point of the LHC where bunches, consisting of approximately 10^{11} protons, collide at a rate of 40 MHz [7]. The number of particles encountered per time is given by [8]

$$\dot{N} = \mathcal{L}\sigma \tag{4.1}$$

with the cross section σ for the present event and the instant luminosity $\mathcal{L}$. Given a measure for the number of collisions per unit time the instant luminosity can be introduced and is often used as key parameter in collider physics [3].

$$\mathcal{L} = \frac{N_b n_b f_{\text{rev}} \gamma_r}{4\pi \epsilon_n \beta^*} F \tag{4.2}$$

Where N_b is the number of particles per bunch, n_b the number of bunches per beam, f_{rev} the rotational frequency, γ_r the Lorentz factor, ϵ_n the normalized transverse beam emittance, β^* the betatron function at the collision point and F respects the geometric luminosity reduction factor due to the crossing angle at the collision point. The design luminosity for ATLAS was exceeded with $\mathcal{L} = 2.05 \times 10^{34}\,\text{cm}^{-2}\,\text{s}^{-1}$ for 2.05 times on the 2$^{\text{nd}}$ of November 2017 emphasizing the great success over the years [9].

The aspiration to be sensitive to the great variety of particles governed by the fundamental forces (see chapter 3.1) influenced the detector design accordingly. The layered structure reflects the fact that The basic structure of ATLAS is shown in figure 4.2 with its different sub-detector systems together with the convention for the used coordinate system. The nominal interaction point acts as origin of the coordinate system where the z-axis follows the beam line. Perpendicular to the z axis lies the transverse x-y-plane usually described through the azimuthal angle ϕ. The positive x-axis points towards the center of the LHC. The cylindric symmetry of the detector suggests a cylindric coordinate system with the angle θ starting from

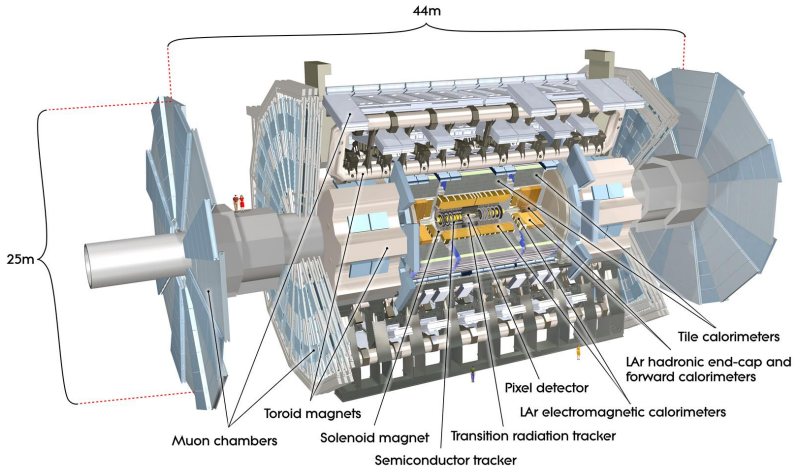

(a) The layered structure of the ATLAS Detector at the LHC with its sub-systems Inner Detector, Calorimeter, magnets and Muon Spectrometer [7].

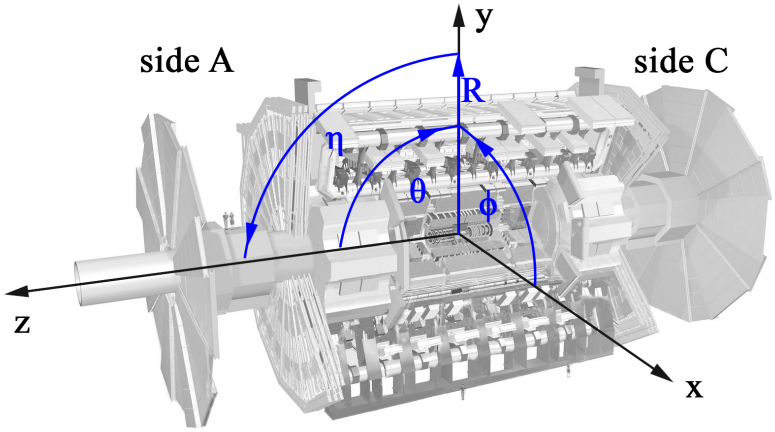

(b) The global ATLAS coordinate system formulated in cylindric coordinates with the z-axis parallel to the beam line and the transverse plane defined through azimuthal angle ϕ and pseudorapidity η. Based on [7].

Figure 4.2: Structure of the ATLAS detector and the used coordinate system.

the beamline. [7] Since the polar angle is not a Lorentz invariant quantity it is useful to describe the position in terms of rapidity [3] $w = \frac{1}{2} \ln \frac{E+p_z c}{E-p_z c}$ in that highly relativistic regime. In the limit of large momenta i.e. $|\mathbf{p}|c \approx E$ the rapidity coincides with the pseudorapidity formulated as [10]

$$\eta = -\ln \tan \frac{\theta}{2} \tag{4.3}$$

This variable has only the polar angle as dependence and is therefore the adequate quantity in the context of collision experiments where usually the angle θ from the beamline is measured. [10]

The magnet configuration includes a superconducting selenoid with a field strength of 2 T sourrounding the inner detector as well as three large superconducting toroid magnets around the calorimeter. The barrel toroid magnet delivers a field strength of 0.5 T and in the end-cap a field of 1 T prevails. [7]
The inner detector is responsible for pattern recognition, momentum and vertex measurements and electrically charged particle identification which is achieved with a combination of semiconductor pixel and microstrip trackers (SCT). Additional straw tube tracking detectors are sensitive to transistion radiation (TRT) in the outer part that are responsible for high vertex and momentum resolution. The $R - \phi$ segmented pixel detectors are of size $50 \times 400\,\mu\text{m}^2$ and the SCTs with its 8 strip layers cover together a range of $|\eta| < 2.5$. Typically 36 hits per track is provided by the 4 mm straw tubes of the TRTs and cover the range $|\eta| \leq 2.0$. [7]
Liquid argon electromagnetic sampling **calorimeter** with high granularity allow an excellent energy performance for electrons and photons. It has a total thickness of more than 22 radiation lengths X_0 in the barrel region ($|\eta| < 1.475$) and more than $24X_0$ in the end-cap region ($1.375 < |\eta| < 3.2$). For hadronic energy measurements a scintillator-tile calorimeter covering $|\eta| < 1.7$ is in operation. It is a sampling calorimeter and uses steel as absorber material and scintillating tiles as active material in conjunction with wavelength shifting fibres. Further LAr technology is used for hadronic particles in the outer pseudorapidity range up to $|\eta| = 3.2$. Here copper plates provide the absorber material. The forward calorimeters extend the coverage for hadronic and electromagnetic energy measurements to $|\eta| = 4.9$ and are $10X_0$ deep. [7]
The **muon system** is suited in the outer layer of ATLAS and provides as independent system resolution for high energy muon tracks with three layered precision chambers. This is possible because of the air-cored toroid magnet system including one barrel and two end-cap magnets generating strong bending power in a large

volume and delivering a mostly perpendicular magnetic field regarding the muon trajectories. The bending power $\int \vec{B}d\vec{l}$ along the muontrack $d\vec{l}$ reaches 1.5 T m to 5.5 T m in the range $|\eta| < 1.4$ (barrel) and up to 7.5 T m (end-cap). The precision chambers are Monitored Drift Tubes (MDT) and in the larger pseudorapidity range Chathode Strip Chambers (CSC) which are multiwire proportional chambers. Due to the fact that the overall performance depends crucially on the alignment of the muon detectors with repect to each other and the Inner Detector MDTs are equipped with a optical monitoring system with 1200 sensors. Resistive Plate Chambers (RPC) and Thin Gap Chambers (TGC) are the constitutes of the muon trigger system. [7]
The data recording rate is limited due to technology and resource limitations and has to be reduced from 40 MHz to 200 MHz. This poses high demands on an efficient **trigger system** which is organised in three levels. Level 1 uses only a subset of the total detector information making basic decisions to flag so called regions of interest i.e. coordinate regions. Searches include patterns for high transverse momenta of muon tracks, electrons and photons as well as jets or large missing energy balances. The output rate after this first selection accounts for 75 kHz. The high level trigger 2 and 3 are responsible for selecting the level 1 triggerd regions at full granularity and precision. The level 3 event filter is the final stage and achieves data reduction down to the final data-taking rate of 200 Hz writing events of the size of approximately 1.3 MB to the disks. The event filter‘s selection criteria are implemented using offline analysis procedures. [7]

4.3 Leptoquark pair production in proton-proton collisions

4.4 b-tagging at ALTAS

The third generation quarks i.e. top (t) and bottom (b) play a crucial role in the Standard Model and its various extension possibilities like the Leptoquark Model due to their large masses [11]. Therefore it is essential to identify hadrons containing b quarks and seperating them from light-flavour quarks at hadron collider detectors like ATLAS. This task is commonly reffered as b-tagging and can be seen as a classi-

fication problem with the goal to assign right jet flavours. Hereby the particle tracks in the Inner Detector and the jet reconstruction of clusters in the electromagnetic and hadronic calorimeter are dicriminating objects. [12]

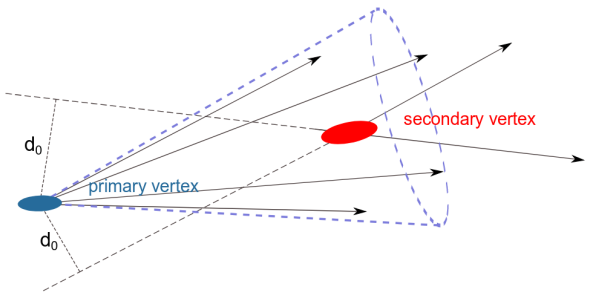

Figure 4.3: Signature of a b-jet with the primary and secondary vertex created relevant for b-tagging. d_0 is the impact parameter. [11]

The long lifetime of B hadrons in the order of 1.6 ps allow them to travel a few millimeters in the detector. The subsequent decay of those heavy particles within a secondary vertex produce tracks with comparably large impact parameter d_0 that is the shortest distance of the particle track from the primary vertex (see figure 4.3). This signature and the deduced impact parameter significance $S(d_0) = \frac{d_o}{\sigma(d_0)}$, where $\sigma(d_0)$ is the uncertainty of the impact parameter, are used by the b-tagging algorithms including five low-level and two high-level taggers. [11] The b-tagging algorithms rely on multivariate combinations of the information and process them to calculate a discriminant value for each jet. Thresholds on these values are then defining the working point to provide efficiencient identification of b-jets. For better information processing of the combinations of large input parameters neural network classes are used. [13] One example for such trained network is the MV2 tagger which uses 24 input variables of the low-level taggers together with kinematic properties*. [12]

*For further detail see [14]

List of Figures

List of Tables

Bibliography

[1] CERN. About CERN. https://home.cern/about. visited on September 4, 2018.

[2] CERN. Cern komplex. http://www.lhc-facts.ch/img/news2015/lhccomplex_.jpg. Last update: October 29, 2011.

[3] Lyndon Evans and Philip Bryant. Lhc machine. *Journal of Instrumentation*, 3(08):S08001, 2008.

[4] The ALICE Collaboration, K Aamodt, et al. The alice experiment at the cern lhc. *Journal of Instrumentation*, 3(08):S08002, 2008.

[5] The LHCb Collaboration, A Augusto Alves Jr, et al. The lhcb detector at the lhc. *Journal of Instrumentation*, 3(08):S08005, 2008.

[6] The CMS Collaboration, S Chatrchyan, et al. The cms experiment at the cern lhc. *Journal of Instrumentation*, 3(08):S08004, 2008.

[7] The ATLAS Collaboration, G Aad, et al. The atlas experiment at the cern large hadron collider. *Journal of Instrumentation*, 3(08):S08003, 2008.

[8] Donald H. Perkins. *Introduction to High Energy Physics* -. Cambridge University Press, Cambridge, 4. aufl. edition, 2000.

[9] Rende Steerenberg. LHC report: LHC reaches 2017 targets. https://home.cern/cern-people/updates/2017/11/lhc-report-lhc-reaches-2017-targets. posted by Stefania Pandolfi on 7 Nov 2017. Last updated 26 Jun 2018, 17.32.

[10] Cheuk-Yin Wong. *Introduction to High-Energy Heavy-Ion Collisions*. WORLD SCIENTIFIC, 1994.

[11] Per Ola Hansson Adrian. The ATLAS b-Jet Trigger. In *Proceedings, 31st International Conference on Physics in collisions (PIC 2011): Vancouver, Canada, August 28-September 1, 2011*, 2011.

[12] Michela Paganini. Machine Learning Algorithms for b-Jet Tagging at the ATLAS Experiment. In *18th International Workshop on Advanced Computing and Analysis Techniques in Physics Research (ACAT 2017) Seattle, WA, USA, August 21-25, 2017*, 2017.

[13] Luca Scodellaro. b tagging in ATLAS and CMS. In *5th Large Hadron Collider Physics Conference (LHCP 2017) Shanghai, China, May 15-20, 2017*, 2017.

[14] Expected performance of the ATLAS b-tagging algorithms in Run-2. Technical Report ATL-PHYS-PUB-2015-022, CERN, Geneva, Jul 2015.